

Study Of Open and Closed Wheels Aerodynamic Of Racing Cars in Wind Tunnels With Movable Ground At Different Car Speeds

Al Muharrami M.S., Almousa S.M., Almutairi A.F.M., Almutairi D.M.S., Coffey M., Martin A., Pereira C., Perks J.L., Stewart E.S., Sultan K.I., Wakefield D.J.W., Wines A.L., Boretti A.A.

School of Science, Information Technology and Engineering,
University of Ballarat, PO Box 663, Ballarat, VIC 3353, Australia

Abstract

The paper proposes the CFD study of a GT2 and a F1 racing car in a wind tunnel with movable ground and wheels. After a sensitivity analysis on the modelling of turbulence and the grid generation parameters, simulations are performed at different air speed to determine the pressure and shear contributions to the lift and drag coefficients. For the GT2 car, the drag and lift coefficients are around $C_D=0.4$ and $C_L=-0.5$ (down force). The down force is mostly the result of the under body diffuser and the rear wing. The rear wing contributes more than 85% of the lift force and 7-8% of the drag force. When reference is made to the low speed drag and lift coefficients, increasing the speed from 25 to 100 m/s produces an increase of C_D of more than 3 % and a reduction of C_L of more than 2 %. For the F1 car, the drag and lift coefficients are strongly variable in between race track and race track, mostly adjusted by the front and rear wing incidence. For the particular set-up, C_D is around 0.8 and C_L is around -1.2 (down force). The down force is mostly the result of the large front and rear wings immediately visible and the under body diffusers and vortex generators hidden below the car. These results suggest modifying the constant C_D and C_L values used in lap time simulation tools introducing the tabulated values to interpolate vs. the speed of the car.

Introduction

In recent years motor racing has become one of the most popular of sports. In all forms of racing, however, aerodynamics is a significant design parameter. The complexity of racing car aerodynamics is comparable to the aerodynamics of airplanes and it is not limited to drag reduction but also to the generation of aerodynamic down force and its effect on cornering speed [1-9, 12-20]. In the process of designing and refining current racing car shapes, all available aeronautics design tools are used including CFD, wind-tunnel testing and track testing. The benefits of aerodynamic down force and the improved performance are basically a result of increasing the tire adhesion by simply pushing the tires more toward the ground. Because of this additional load, larger friction (traction) levels can be achieved, and the vehicle can turn, accelerate, and brake more quickly. By controlling the fore/aft down force ratio, vehicle handling can be easily modified to meet the needs of a particular race track. Down force may be generated by adding inverted wings or by using the vehicle body. Even small values of negative pressure under the vehicle can result in a sizable aerodynamic down force because of the large plan view area of the vehicle. The large front and rear wings are immediately visible. Under body diffusers and vortex generators are hidden below the car. Front wings operate very close to the ground, resulting in a significant increase in down force. This significant increase is due to the wing-in-ground effect. The effect does not come freely because a similar increase in drag is measured. Front

wings mounted close to the ground are widely utilized in race-car design. Large rear wings are also commonly used. These wings have very small aspect ratio (span/chord ratio). The small aspect ratio translates in a significantly high drag, but with a delayed wing stall. This penalty is reduced by adding very large end plates improving the lift-to-drag ratio.

Race-car wings exhibit a strong interaction between the lifting surface and the other body components. The combined down force increases as the wing approaches the vehicle's rear deck. At a very close proximity the flow separates between the rear deck and the wing and the down force is reduced. The horizontal positioning (such as fore-aft) of the wing also has a strong effect on the vehicle's aerodynamics and usually down force increases as the wing is shifted backward. The very large change in the down force is due to the increased under body diffuser flow. Creating down force with the vehicle's body is a very well known concept since Colin Chapman designed the famous Lotus 78 where the vehicle's side pods had an inverted airfoil shape and the two sides of the car were sealed by sliding skirts to produce large down forces. Once the sliding skirts were banned the suction under the car was significantly reduced. A logical evolution of this concept led to under body tunnels formed under the side pods. The fore-aft shifting of the diffuser entrance also controls the location of the vehicle's centre of pressure through the pressure peak at the entrance. The down force usually increases with reduced ground clearances. Simple modifications can be added to an existing car to increase down force. One of the simplest add-ons is the vortex generator, usually small triangular plates or miniature wings. Adding such vortex generators at the front of the under body where their long vortex trails can induce low pressure under the vehicle.

The computational domain is made of the wind tunnel and the car. The computational domain is bounded by inlet, outlet, ground, left, right and ceiling boundaries and by the car. The wheels of the car are moving as well as the ground changing the flow pattern under the body of the car resulting in significantly different lift and drag coefficients vs. the fixed ground and fixed wheels traditional wind tunnel experiments [1]. Simulations are performed with the STAR-CCM+ code [10]. Star-CCM+ is extensively used by many racing car departments. This code may tackle problems involving multi-physics and complex geometries producing results with minimum user effort. STAR-CCM+ fits easily within engineering process and allow automating the simulation workflow and performing iterative design studies with minimal user interaction.

The grid size is very well known to affect the results, because this kind of industrial problems is clearly grid dependent. Especially the shear contributions are expected to change significantly with the grid size, while the pressure contributions are expected to change less. The turbulence modelling is

expected to change especially the shear contributions. However, in case of more significant separated flows, the turbulence modelling may change also the pressure contribution in a significant extent. This paper studies the influence of the turbulence modelling on the computed drag and lift coefficients with grid densities of the order of 1 to 3 million cells for half the model, the minimum cell refinement to produce acceptable results even if not grid independent results [10, 27-30] for general aerodynamics.

Turbulence is then modelled with the most popular one and two equations models, those making more sense with the adopted refinement, coupled to a Reynolds Averaged Navier-Stokes (RANS) solution. The Spalart-Allmaras model (SA here after) is the simplest model considered, and may therefore fails to reproduce the effects of turbulence up to an acceptable level of accuracy. The SA turbulence models solve a single transport equation that determines the turbulent viscosity [21-23]. The model is not well suited to applications involving jet-like free-shear regions [23]. It is also likely to be less suited to flows involving complex recirculation and body forces (such as buoyancy) than two-equation models such as K- ϵ and K- ω . The realizable two layers K- ϵ model (k- ϵ here after) is a much more sophisticated model providing satisfactory results in many more applications of practical interests even if within the limits of a two equations model. The K- ϵ model adopted here is the realizable all y+ Two-Layer K- ϵ Model [24-25]. The SST K- ω model (k- ω here after) is a similarly sophisticated model providing satisfactory results in a significant number of applications of practical interests even if within the same limits of a two equations model [23]. The K- ω model adopted here is the SST K- ω model [26]. The SST model has seen fairly wide application in the aerospace industry, where viscous flows are typically well resolved and turbulence models are generally applied throughout the boundary layer but is possibly less reliable than the realizable all y+ Two-Layer K- ϵ Model.

Closed wheels GT2 car model

The GT2 cars are very close to street cars, differing at the most for the under body of the car that is flat and the downstream diffuser also flat. The GT2 aerodynamic is much less sophisticated than in other classes, for example Le Mans Racing Series cars, where there are many more opportunities to optimize drag and lift coefficients and consequently more complex fluid dynamic problems to be addressed. The computational mesh is made up of 0.9 million cells for half the model (880009 cells, 2581088 faces, 1048242 verts). The equivalent full model resolution is 1.8 million cells. The unstructured mesh is refined close to the car body, in the wake and in the region under the car.

Figure 1 presents the contour plots for velocity on the symmetry plane for the k- ω simulations at different car speeds. The pressure contours are very close each other, proving the assumption of constant C_D and C_L are generally a fair assumption to then compute the drag and lift forces of the car at different speeds. Table 1 presents the drag and lift coefficients obtained at different car speeds with the three turbulence models k- ω , k- ϵ and SA with movable ground and rotating wheels. The level of reduction of residuals is the same for all the simulations. The wall y+ changes over the car body from values of the order of 0.1 to values above 1000. The rear wing is the major source of down force, accounting for more than 80% of the lift coefficient. The under body of the car is responsible for less than the 20% of the lift coefficient. The penalty in drag due to the rear wing (without considering the supports) is about a 7-8%.

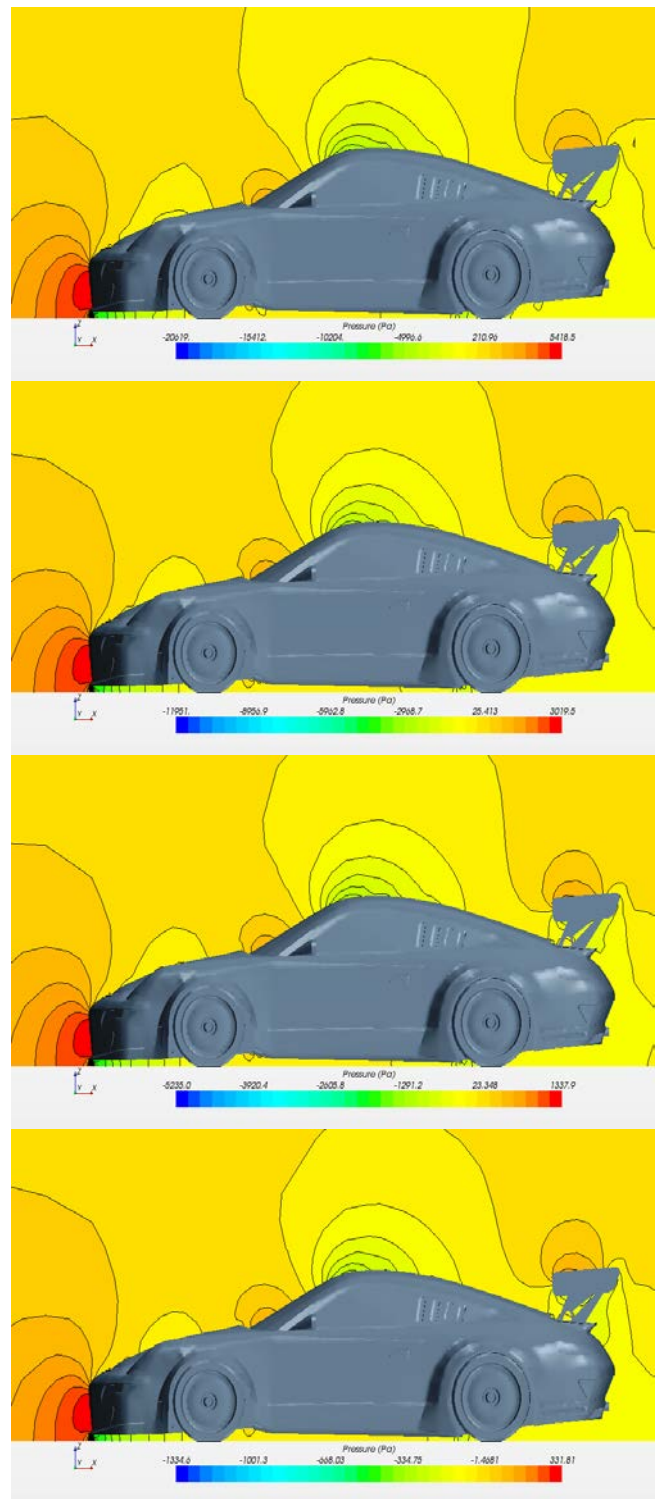


Figure 1 – GT2 car - Velocity contour plots at 100, 75, 50 and 25 m/s speed with movable ground and k- ω modelling.

The accuracy of the low speed assumption is more than reasonable, being the car aerodynamic on the track also affected by other factors like wakes and uneven ground. Changing the speed, both the Mach and the Reynolds number change. The Mach number influence is negligible. The Reynolds number influence is also modest. The shear C_D reduces increasing the velocity, but the shear contribution to C_D is minimal if compared to the pressure contribution that is about constant. The same is true for the shear C_L . The module of the negative pressure C_L is also reducing increasing the velocity. The k- ω and k- ϵ models produce pretty much the same results, even if the C_D is generally

slightly larger with the $k-\omega$ while the module of the C_L is generally slightly larger with the $k-\epsilon$. The SA model performs quite well especially for what concerns the C_D , while the module of the C_L is generally underestimated. Within the routine computations of aerodynamic changes by using 1.2-1.5 million cells unstructured meshes for half a car (2.4-3 million cells total), it is therefore reasonable to use either the $k-\omega$ or the $k-\epsilon$ model of turbulence for race car optimisation, while the SA is possibly compromising the computation of the lift coefficient.

Speed [m/s]	25	50	75	100	
C_D total	4.19E-01	4.22E-01	4.27E-01	4.18E-01	k- ω
C_D shear	2.37E-02	2.16E-02	2.01E-02	1.96E-02	
C_D pressure	3.95E-01	4.01E-01	4.07E-01	3.99E-01	
C_L total	-4.73E-01	-4.66E-01	-4.61E-01	-4.46E-01	
C_L shear	5.01E-03	4.39E-03	4.10E-03	3.85E-03	
C_L pressure	-4.78E-01	-4.70E-01	-4.65E-01	-4.50E-01	k- ϵ
C_D total	4.12E-01	4.14E-01	4.15E-01	4.12E-01	
C_D shear	2.62E-02	2.38E-02	2.23E-02	2.18E-02	
C_D pressure	3.86E-01	3.90E-01	3.93E-01	3.90E-01	
C_L total	-4.79E-01	-4.82E-01	-4.77E-01	-4.71E-01	
C_L shear	5.37E-03	4.86E-03	4.56E-03	4.32E-03	SA
C_L pressure	-4.85E-01	-4.87E-01	-4.82E-01	-4.75E-01	
C_D total	4.13E-01	4.23E-01	4.30E-01	4.25E-01	
C_D shear	1.40E-02	1.32E-02	1.25E-02	1.17E-02	
C_D pressure	3.99E-01	4.10E-01	4.18E-01	4.13E-01	
C_L total	-4.49E-01	-4.48E-01	-4.21E-01	-4.31E-01	
C_L shear	1.19E-03	9.64E-04	7.73E-04	7.01E-04	
C_L pressure	-4.50E-01	-4.49E-01	-4.22E-01	-4.32E-01	

Table 1 – Lift and drag coefficient results for the GT2 car.

Open wheels F1 car model

Simulations have then been performed for a F1 racing car. This open wheels car is very far from street cars and has a very complex aerodynamics. The 1.35 m mesh has 1346427, 4009724 and 1587546 cells, faces and verts. The 2.63 m mesh has 2628665, 7803413 and 3076430 cells, faces and verts. The equivalent full model resolutions are 3.70 m and 5.3 m cells respectively. The unstructured mesh is refined close to the car body, in the wake and in the region under the car. The mesh refinement is much better than the one adopted for the GT2 car. However, the aerodynamics is now much more complex, and this level of mesh refinement may be not enough to capture all the most relevant features affecting the drag and lift phenomena. The wall y^+ changes over the car body from values of the order of 0.1 to values above 1000.

Figure 2 presents the computed stream lines around the body of the car and the contour plots for pressure and velocity magnitude on the symmetry plane obtained at 90 m/s with the movable ground and rotating wheels by using the $k-\epsilon$ solver. Table 2 presents the results obtained for the total drag and lift forces with the $k-\omega$, $k-\epsilon$ and SA models same speed, movable ground and rotating wheels, and 2 mesh refinements. The level of reduction of residuals is the same for all the simulations. Clearly, for these cars with a much more complex aerodynamics made of separate jet flows the turbulence model is of paramount importance to the proper computation especially of the lift coefficient. The drag and lift coefficients are possibly underestimated by the SA. The lift coefficient is much larger in module with the $k-\epsilon$ model than the $k-\omega$ and the SA (+25-35%). This is mostly due to the much different pressure distribution around the car obtained with the $k-\epsilon$. This result tells us that the 2 most reliable models, the $k-\epsilon$ and the $k-\omega$, provide in this case better results than the SA, but there is still a large discrepancy in between the $k-\omega$ and the $k-\epsilon$ that deserves further investigation. Better mesh refinement may certainly reduce the discrepancies between the $k-\epsilon$ and the $k-\omega$ results.

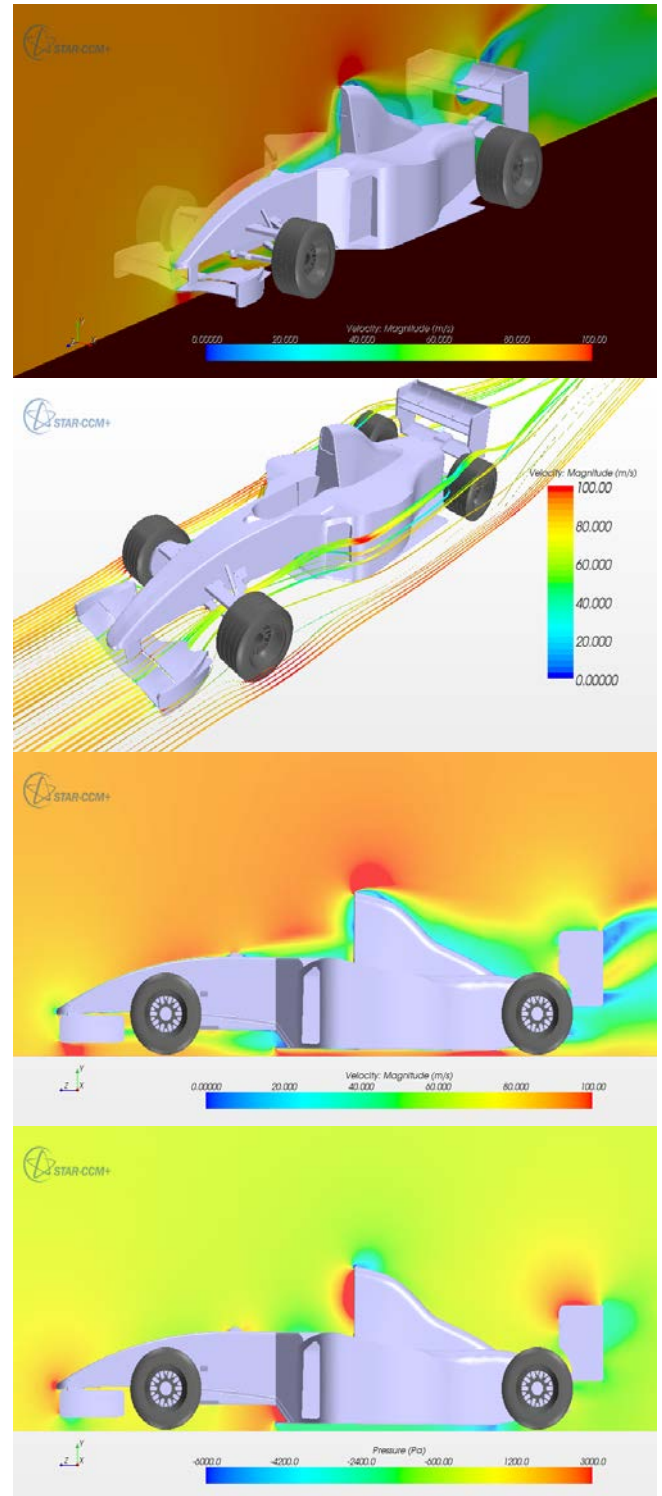


Figure 2 – F1 car - Streamlines and velocity and pressure contour plots at 90 m/s speed with movable ground, $k-\epsilon$ modelling and 1.35 million cells mesh half model.

For open wheels cars the minimum mesh requirements for a reasonable accuracy is possibly 4 times finer than the one adopted. The erratic behaviour may be certainly reduced increasing the number of mesh points. However, simulations done by increasing the mesh size from 1.35 to 2.63 million cells half model do not show any improvement as shown in Table 2. Low speed wind tunnel measurements of drag and lift forces on a model car without moving ground and wheels have shown the down force exceeding the drag force by a 40%. We may therefore conclude that the $k-\epsilon$ has a better accuracy than the $k-\omega$

and the SA models for this kind of applications dealing better with the mostly separated flows.

Mesh size	1.35m	1.35m	2.63m	
Speed [m/s]	45	90	45	
C_D total	7.57E-01	7.55E-01	7.58E-01	k- ω
C_D shear	2.48E-02	2.20E-02	2.52E-02	
C_D pressure	7.32E-01	7.33E-01	7.32E-01	
C_L total	-7.64E-01	-8.00E-01	-7.11E-01	
C_L shear	9.26E-04	9.40E-04	4.63E-04	
C_L pressure	-7.64E-01	-8.01E-01	-7.12E-01	
C_D total	7.97E-01	7.83E-01	8.01E-01	k- ϵ
C_D shear	3.44E-02	3.04E-02	3.53E-02	
C_D pressure	7.62E-01	7.52E-01	7.65E-01	
C_L total	-1.15E+00	-1.08E+00	-1.16E+00	
C_L shear	2.00E-05	-2.27E-04	-4.29E-04	
C_L pressure	-1.15E+00	-1.08E+00	-1.16E+00	
C_D total	7.85E-01	7.45E-01		SA
C_D shear	2.17E-02	1.99E-02		
C_D pressure	7.63E-01	7.25E-01		
C_L total	-7.59E-01	-7.33E-01		
C_L shear	-9.73E-04	-7.72E-04		
C_L pressure	-7.58E-01	-7.33E-01		

Table 2 – Lift and drag coefficient results for the F1 car.

Conclusions

The aerodynamic of racing cars can be improved by using computational fluid dynamic (CFD) tools. These tools provide results quite accurate within very short time scales. Results of simulations are generally not grid independent and not model independent. However, once these limitations are properly understood, these tools may be used to reduce the design cycle that must also rely on wind tunnel and track testing. Without validation, results of simulations are indeed of no value.

The set of results and observations included in this report suggests that CFD can be a very useful tool to support the aerodynamic design of race cars. The most important requirement for the production of accurate results is the mesh resolution, with a minimum advised for any calculations looking to determine the aerodynamic forces produced by the vehicle increasing with the complexity of the car aerodynamic. If 1.2-1.5 million cells are reasonable for close to street cars configurations with closed wheels (the GT2 example), these meshes are not fine enough for open wheels as the F1 example.

The choice of the appropriate turbulence model needs further investigation, as the different available formulations were not applied to the large meshes. However, the predicted flow patterns suggest that the specific k- ω and k- ϵ models perform better when predicting the separation point on the aerodynamic surfaces and when dealing with transition and separation effects in general than the basic k- ω and k- ϵ models as well as SA models. The addition of a transition model to these calculations could greatly improve the results.

With the evolution of computational power and mesh generation algorithms, larger and better quality grids will be available increasing the quality of the simulations. It is then left to the designers to find the balance between the number of simulations they are able to run and the accuracy of these calculations. As the technology evolves, the importance of numerical methods in race car design is likely to increase, although experimental methods are still needed.

References

[1] J. Katz, *Race-Car Aerodynamics*, 2d ed., Robert Bentley Inc., Cambridge, Massachusetts, 2006

[2] J. Katz, *Aerodynamics of race cars*, Annual Review Fluid Mechanics, 38:27–64, 2006.

[3] W. F. Milliken and D. L. Milliken, *Race Car Vehicle Dynamics*, SAE International, Warrendale, Pennsylvania, 1995.

[4] J. P. Brzustowicz, T. H. Lounsberry, and J. M. Esclafer de la Rode, *Experimental and Computational Simulations Utilized During the Aerodynamic Development of the Dodge Intrepid R/T Race Car*, SAE P. 2002-01-3334.

[5] L. T. Duncan, *Wind Tunnel and Track Testing an ARCA Race Car*, SAE P. 901867.

[6] F. K. Schekel, *The Origins of Drag and Lift Reductions on Automobiles With Front and Rear Spoilers*, SAE P. 77-0389.

[7] mhest.com/spotlight/automobiles/articles/Race-CarAerodynamics.pdf

[8] www.nas.nasa.gov/About/Education/Racecar/glossary.html

[9] www.bosch-motorsport.com/content/downloads/Software/ManualLapSimV2007.pdf

[10] www.cd-adapco.com/products/star_ccm_plus/index.html

[11] www.chassissim.com

[12] M. J. Williams, *Validation of CFD for Racing Car Analysis and Design*, SAE P. 2002-01-3349.

[13] R. Singh, *CFD Simulation of NASCAR Racing Car Aerodynamics*, SAE P.2008-01-0659.

[14] D. Ueno, G. Hu, I Komada, K. Otaki, Q. Fan, *CFD Analysis in Research and Development of Racing Car*, SAE P. 2006-01-3646.

[15] A. De Vita, L. Di Angelo, L. Andreassi, S. Romagnuolo, *CFD-Aided Design of an Airbox for Race Cars*, SAE P. 2002-01-2167.

[16] C. Connor, A. Kharazi, J. Walter, B. Martindale, *Comparison of Wind Tunnel Configurations for Testing Closed-Wheel Race Cars: A CFD Study*, SAE P. 2006-01-3620.

[17] B. D. Duncan, K. Golsch, *Characterization of Separated Turbulent Flow Regions in CFD Results for a Pontiac NASCAR Race Car*, SAE P. 2004-01-3556.

[18] E. Duell, C. Connor, B. Martindale, J. Walter, S. Arnette, *Advantages of Adaptive Wall Wind Tunnel Technology: A CFD Study for Testing Open Wheel Race Cars*, SAE P. 2007-01-1048.

[19] S. Desai, E. Leylek, C. B. Lo, P. Doddegowda, A. Bychkovsky, A. R. George, *Experimental and CFD Comparative Case Studies of Aerodynamics of Race Car Wings, Underbodies with Wheels, and Motorcycle Flows*, SAE P. 2008-01-2997.

[20] A. P. Mears, R. G. Dominy, *Racing Car Wheel Aerodynamics – Comparisons between Experimental and CFD Derived Flow-Field Data*, SAE P. 2004-01-3555.

[21] Spalart, P.R., and Allmaras, S.R. 1992. *A one-equation turbulence model for aerodynamic flows*, AIAA-92-0439.

[22] Baldwin, B.S. and Lomax, H. 1978. *Thin-Layer Approximation and Algebraic Model for Separated Turbulent Flows*, AIAA-78-0257.

[23] Wilcox, D.C. 1998. *Turbulence Modeling for CFD*. 2nd edition, DCW Industries, Inc.

[24] Shih, T.-H., Liou, W.W., Shabbir, A., Yang, Z. and Zhu, J. 1994. *A New k- ϵ Eddy Viscosity Model for High Reynolds Number Turbulent Flows - Model Development and Validation*, NASA TM 106721.

[25] Rodi, W. 1991. *Experience with Two-Layer Models Combining the k- ϵ Model with a One-Equation Model Near the Wall*, 29th Aerospace Sciences Meeting, January 7-10, Reno, NV, AIAA 91-0216.

[26] Menter, F.R. 1994. *Two-equation eddy-viscosity turbulence modeling for engineering applications*, AIAA Journal 32(8) pp. 1598-1605.

[27] www.cd-adapco.com/pdfs/presentations/eu10/VOLVO_TECH.pdf

[28] www.cd-adapco.com/pdfs/presentations/eu10/ORECA.pdf

[29] www.cd-adapco.com/events/webinars/7014000000N0KQAA0

[30] www.cd-adapco.com/pdfs/presentations/avt09/01_UC_Dec2009_VSim_ho.pdf